IEEE Access
Multidisciplinary | Rapid Review | Open Access Journal

Received July 16, 2019, accepted August 15, 2019, date of publication August 23, 2019, date of current version September 5, 2019.

Digital Object Identifier 10.1109/ACCESS.2019.2937127

Unidirectional Light Scattering With High *f* /*b* at Optical Frequencies Based on Coupled Nanoantennas

DENGCHAO HUANG, YI ZHANG, AND LISHENG YANG
Laboratory of Aerocraft Tracking, Microelectronics and Communications Engineering, Chongqing University, Chongqing 400044, China
Corresponding author: Lisheng Yang (ylscqu@sina.com)

ABSTRACT We propose an optically coupled nanoantenna which contains an asymmetric dimer of core-dual shells nanoparticles, and the individual nanoparticle consisting of two identical metal strips that separated by a dielectric spacer known as the metal-dielectric-metal (MDM) structure. According to the dipole-dipole theory and the Mie theory, we theoretically and numerically demonstrate that this design can provide unidirectional forward scattering along the incident axis of light with high *f* /*b* radio (known as the ratio of scattering spectra to forward and backward direction) and narrow beam-width owing to interference between electric dipole and magnetic high-order modes. We also find that all properties of this nanoantenna that the performance of it is related with the gap separation of the asymmetric dimer. Comparing with the asymmetric dimer of pure metal nanoparticles and the symmetric dimer of MDM nanoparticles, the proposed nanoantenna has higher directivity and low loss at the same time, due to effectively coupled electric dipole mode and magnetic multipole modes. The ultra-directional nanoantenna may shed new light to overcome power losses and low directivity of coupled nanoantennas, which can find various applications in bio-sensing and metamaterials.

INDEX TERMS Coupled nanoantenna, core-dual shells nanoparticle, dipole-dipole theory, Mie theory.

I. INTRODUCTION

Nanoantennas which can control the directionality of scattered electromagnetic waves at optical frequencies have attracted tremendous attention. The ability of effectively converting the localized electromagnetic field into freely propagating light in the desired direction makes directional nanoantennas highly desirable for many applications (e.g., optical communications, nonlinear optics, biosensing, photovoltaics, astrophysics and material technology [1]–[7]). Nanoantennas made of metal nanoparticles are able to effectively convert the collected light into freely propagating light in the desired direction even below the diffraction limit due to the collective oscillations behavior of the free electrons near the surface of the metal, called localized surface plasmon resonances which confine the electric field into a subwavelength area [8], [9]. As one well-known example is one of the first Yagi-Uda optical nanoantenna consisting of several metal particles, which can strongly enhance the directivity was successfully manufactured, due to the excitation of localized surface plasmons resonance at the metallic interfaces and strong field enhancement near the feed element [10]. More and more compact structures such as metallic particle and V-shaped metallic nanostructures can support unidirectional scattering and near electric field enhancement in the gap due to coupled electric and magnetic multipolar resonances excited in the particles [11], [12]. However, these applications have been restrained since of large lossy of metals. Recently, dielectric and core-shell nanostructures have been presented and as good candidates to metallic nanostructures in many applications [13]–[16], owing to their lower losses and their abilities to support both electric and magnetic modes [15], [17]. Liu [18]. demonstrated that a core-shell nanoparticle consisting of a dielectric shell and a metal core can allow flexible overlapping electric and magnetic multipole of high orders which were excited by a plane wave, which results in significantly narrow radiation beam-width and backward scattering suppression, and Zhang *et al.* [19]. also show that a local dipole source can efficiently excite several hybridized plasmonic modes in multilayered nanoantennas, which lead to unidirectional emissions in opposite directions at different wavelengths. However, comparing with

The associate editor coordinating the review of this article and approving it for publication was Rahul A. Trivedi.

these nanoantennas consisting of an individual nanoparticle, these coupled nanostructures would have better scattering property and high scattering intensity.

Nanoantennas consisting of plasmonic [12], [20] or dielectric [21], [22] coupled nanoparticles with nanoscale gaps have shown tremendously strong field confinement and enhancement in the gap. Nevertheless, the metal nanoantenna is known to be large power absorption and substantial energy loss at the optical frequency and the dielectric one need strong coupling to support efficient directional forward scattering. To overcome these disadvantages, a novel type of optical nanoantenna made of two coupled core-dual shells (metal-dielectric-metal) particles is proposed in this paper. The multiple layers of the nanoparticle can achieve both electric and magnetic multipole of high-orders, and the metallic surface has been provided to know enhancement of the magnetic dipole emission and suppression of the electric dipole emission [23]–[25]. And the dielectric layer can also support magnetic resonances which show a strong far-field scattering, deriving from the rotation of the displacement current inside it [26], [27]. Albella *et al.* [20] theoretically and numerically demonstrated that compared with the coupled symmetric metal nanoparticles, the coupled symmetric dielectric dimer has better capabilities of magnetic field-enhancing, directional emission and quantum efficiency. Furthermore, Shibanuma *et al.* [21] support that the asymmetric dielectric dimer has the better f/b ratio and maximum forward scattering efficiency than the symmetric dielectric dimer when the separation gap of the particle increase.

In this paper, the asymmetric dimer of MDM nanoparticles has been shown as a solution to attain high f/b ratio and narrow beam-width. For light sensing and imaging applications, optical antennas should collect incident light efficiently and control it in a desirable direction [34], [35]. That means this nanoantenna consisting of the coupled MDM particles with high f/b ratio and narrow beam-width can scatter the incident light into the desirable direction efficiently with low scattering power in other direction. Such effective light collection and the strong light focusing effect can not only enhance the photoresponsivity of a photodetector through the effective light collection, but also enable high-resolution light sensing and imaging.The resonant frequencies of this nanostructures are tunable by changing the dimension of the MDM nanoparticle.Comparing the dielectric dimer, this MDM dimer can offer high directivity by exciting electric resonance in one particle and the magnetic resonance in the other one, when these two particles are not placed close to each other. This study uses a detailed theoretical analysis of the asymmetric dimer of MDM nanoparticles based on the dipole-dipole theory [20] and the Mie theory [28]. The phenomenon of Fano resonance has been observed [29], which results from the interference between the significantly broadened electric dipole and the nearly unbroadened magnetic dipole of the coupled core-shells particles. The paper is organized as follows. In Section 2, the model of the asymmetric dimer of core-dual shells particles is proposed based on the dipole-dipole theory [20] and the Mie theory [28], and the corresponding structural parameters are confirmed by adopting the method of a local optimum. In Section 3, the radiation characteristics of the asymmetric dimer irradiated are investigated by a plane wave is shown. Furthermore, the radiation performances of the asymmetric dimer and symmetric dimer for the same geometry with different separations gap are also investigated. Our conclusions are summarized in the last section.

II. SIMULATION MODEL AND METHODS

A. SIMULATION MODEL

The individual MDM nanoparticle can be turned to support both electric and magnetic dipolar or multipolar responses due to the generation of intense displacement currents in the dielectric layer and the collective polarization of conduction electrons in metal layers when it is excited by the plane wave. Therefore when the MDM nanoparticles are coupled together to form the asymmetric dimer, they can provide field enhancement, localization of electromagnetic energy in the gap and high forward scattering intensity with narrow beam-with. In addition, we thus analyze the properties of the asymmetric dimer consisting of two spheres, which is shown in Fig. 1. Numerical simulations are carried out using the CST Microwave Studio software to support the optical responses of the asymmetric dimer in air. For the asymmetric dimer in air, a plane wave as the excitation source with polarization perpendicular to the dimer axis is used to calculate the scattered field. The structure of each sphere can keep their resonances in the low absorption range of the spectrum. In our work, we choose high-permittivity germanium (Ge) as the middle layer of the nanoparticle. The constant permittivity of germanium $\varepsilon = 16.8$ and dissipative loss in germanium

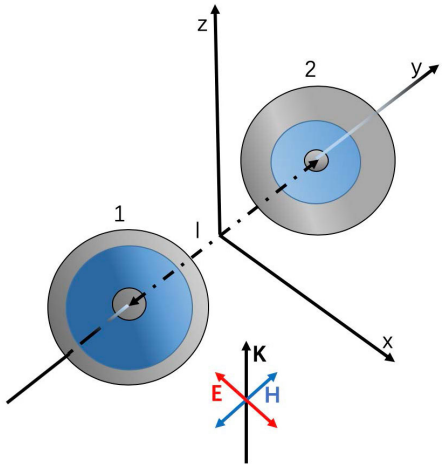

FIGURE 1. Schematic representation of an asymmetric dimer of core-dual shells MDM particles showing the incoming radiation and its electric and magnetic polarization (along the x-axis). Both spheres have three layers of materials (Ag-Ge-Ag), from left to right the radius of the core is $r_{c1} = 40$ nm, $r_{c2} = 25$ nm respectively; the radius of the middle shell is $r_{m1} = 200$ nm, $r_{m2} = 100$ nm respectively; and the radius of the outmost shell is $r_{o1} = 225$ nm, $r_{o2} = 230$ nm respectively, the center to center separation is l.

is very low in the work spectrum [30]. For the dispersion of silver core and shell, we adopt the Drude model , with plasma frequency $\nu_p = 2180$ THz and collision frequency $\gamma = 4.93$ THz [30].

B. THEORETICAL ANALYSES

We displace the dimer consisting of two MDM spheres which are illuminated by a plane wave with electric polarization perpendicular to the dimer axis in the air. We use the dipole-dipole model [20] to analyses the extinction cross-section of the dimer. The extinction cross-section in the forward direction is given by :

$$\delta_{ext} = \frac{4\pi}{kE_0} Im\left(2\frac{k^2}{4\pi\varepsilon_0\varepsilon_h}p_{1x} - 2Z\frac{k^2}{4\pi\varepsilon_0\varepsilon_h}m_{1y}\right) \quad (1)$$

where k is the angular wave number in the background (it is the vacuum in our study),ε_0, and ε_h are the permittivity of vacuum, and the surrounding medium, respectively. Z is the vacuum impedance. In addation, p_{1x} and m_{1y} indicate the induced electric and magnetic dipole moments, respectively. When the incident plane wave is polarised along the x axis, the response of the electric and magnetic dipole moments can be given as:

$$p_{1x} = \varepsilon_0\varepsilon_h\alpha_{1e}E_0 + \alpha_{1e}k^2 g_{xx}p_{2x} \quad (2)$$
$$p_{2x} = \varepsilon_0\varepsilon_h\alpha_{2e}E_0 + \alpha_{2e}k^2 g_{xx}p_{1x} \quad (3)$$
$$p_{1z} = -\alpha_{1e}k^2 g_{yy}p_{2z} + i\varepsilon_0\varepsilon_h\alpha_{1e}Zk^2 g_{zy}m_{2y} \quad (4)$$
$$p_{2z} = -\alpha_{2e}k^2 g_{yy}p_{1z} - i\varepsilon_0\varepsilon_h\alpha_{2e}Zk^2 g_{zy}m_{1y} \quad (5)$$
$$m_{1y} = -\frac{\alpha_{1m}}{Z}E_0 + i\frac{\alpha_{1m}}{Z}\frac{k^2}{\varepsilon_0\varepsilon_h}g_{zy}p_{2z} - \alpha_{1m}k^2 g_{yy}m_{2y} \quad (6)$$
$$m_{2y} = -\frac{\alpha_{2m}}{Z}E_0 - i\frac{\alpha_{2m}}{Z}\frac{k^2}{\varepsilon_0\varepsilon_h}g_{zy}p_{1z} - \alpha_{2m}k^2 g_{yy}m_{1y} \quad (7)$$

where p_{jx} and p_{jz} are the electric dipole moments excited in the jth ($j = 1,2$) sphere along the x-axis and the z-axis, respectively, m_{jy} is a magnetic dipole along the y-axis, g_{xx} , g_{yy} and g_{zy} are the scalar green functions. α_{je} and α_{jm} are the electric and magnetic dipoles respectively, in the three layers sphere can be calculated as formulation (8), (9), shown at the bottom of this page.

Ricatti-Bessel functions are calculated by (10) :

$$\psi_n(z) = zj_n(z),\ \chi_n(z) = -zy_n(z),\ \xi_n(z) = zh_n^{(1)}. \quad (10)$$

$h_n{}^{(1)} = j_n(z) + iy_n(z)$ is the spherical Hankel function of the first classA_n^3 and B_n^3 can be realized as material and geometrical properties of these three layers spheres which are calculated by (11), (12), shown at the bottom of this page.

A_n^2 and B_n^2 are:

$$A_n^{(2)} = \frac{m_2\psi_n(m_2x_1)\psi_n'(m_1x_1) - m_1\psi_n'(m_2x_1)\psi_n(m_1x_1)}{m_2\psi_n{}'(m_1x_1)\chi_n(m_2x_1) - m_1\chi_n{}'(m_2x_1)\psi_n(m_1x_1)} \quad (13)$$

$$B_n^{(2)} = \frac{m_2\psi_n(m_1x_1)\psi_n{}'(m_2x_1) - m_1\psi_n{}'(m_1x_1)\psi_n(m_2x_1)}{m_2\chi_n{}'(m_2x_1)\psi_n(m_1x_1) - m_1\psi_n{}'(m_1x_1)\chi_n(m_2x_1)} \quad (14)$$

among them $x_l = kr_l$ and $m_l = \sqrt{\varepsilon_l/\varepsilon_0}$.

III. RESULTS AND DISCUSSION

We investigated the asymmetric dimer of MDM spheres, which is shown in Fig. 1, in air using the CST Microwave Studio software to support the optical responses. The scattering cross-section of the forward and backward direction and the f/b ratio for two individual particles and the asymmetric dimer of MDM particles are shown in Fig. 2a-c. These two MDM spheres, which structure parameters are given in section I, couple in air and forming the asymmetric dimer. In this study, we can get the peak of the scattering cross-section with the high f/b radio (about 40) while these two particles are not closed to each other ($l = 40$ nm). These coupled spheres are illuminated by a plane wave polarized perpendicular to the particle axis. These two distinctly broad peaks are observed around $f = 750$ THz and $f = 790$ THz, and around $f = 680$ THz and $f = 750$ THz in the scattering spectra, which correspond to the magnetic and electric dipolar resonances of the large and small particles, respectively. Compared with dipole resonances, multipolar resonances are observed at higher frequencies. In the f/b ratio spectra of these two single MDM spheres, several peaks are observed at frequencies. The value of it is higher than electric dipole

$$\alpha_e = \frac{\psi_n(x_3)[\psi_n'(m_3x_3) - A_n^{(3)}\chi_n'(m_3x_3)] - m_3\psi_n'(x_3)[\psi_n(m_3x_3) - A_n^{(3)}\chi_n(m_3x_3)]}{h_n^{(1)}(x_3)[\psi_n'(m_3x_3) - A_n^{(3)}\chi_n'(m_3x_3)] - m_3(h_n^{(1)}(x_3))'[\psi_n(m_3x_3) - A_n^{(3)}\chi_n(m_3x_3)]} \quad (8)$$

$$\alpha_m = \frac{m_3\psi_n(x_3)[\psi_n{}'(m_3x_3) - B_n^{(3)}\chi_n'(m_3x_3)] - \psi_n{}'(x_3)[\psi_n{}'(m_3x_3) - B_n^{(3)}\chi_n(m_3x_3)]}{m_3h_n^{(1)'}(x_3)[\psi_n{}'(m_3x_3) - B_n^{(3)}\chi_n'(m_3x_3)] - h_n^{(1)'}(x_3)[\psi_n{}'(m_3x_3) - B_n^{(3)}\chi_n(m_3x_3)]} \quad (9)$$

$$A_n^{(3)} = \frac{m_3\psi_n(m_3x_2)[\psi_n'(m_2x_2) - A_n^{(2)}\chi_n'(m_2x_2)] - m_2\psi_n'(m_3x_2)[\psi_n(m_2x_2) - A_n^{(2)}\chi_n(m_2x_2)]}{m_3h_n^{(1)}(m_3x_2)[\psi_n'(m_2x_2) - A_n^{(2)}\chi_n'(m_2x_2)] - m_2h_n^{(1)'}(m_3x_2)[\psi_n(m_2x_2) - A_n^{(2)}\chi_n(m_2x_2)]} \quad (11)$$

$$B_n^{(3)} = \frac{m_2\psi_n(m_3x_2)[\psi_n{}'(m_2x_2) - B_n^{(2)}\chi_n'(m_2x_2)] - m_3\psi_n{}'(m_3x_2)[\psi_n(m_2x_2) - B_n^{(2)}\chi_n(m_2x_2)]}{m_2h_n^{(1)'}(m_3x_2)[\psi_n{}'(m_2x_2) - B_n^{(2)}\chi_n'(m_2x_2)] - m_3h_n^{(1)'}(m_3x_2)[\psi_n(m_2x_2) - B_n^{(2)}\chi_n(m_2x_2)]} \quad (12)$$

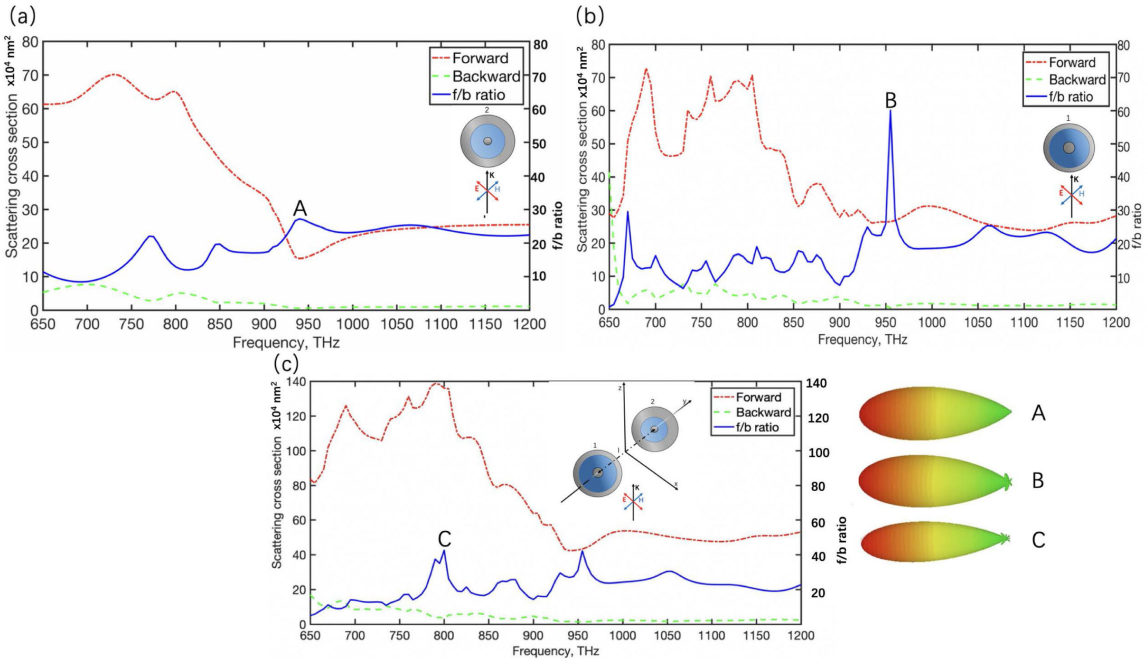

FIGURE 2. Structures and results of the CST simulation. (a-c) the scattering cross section to the forward and backward direction and the f/b ratio of the 230 nm diameter single MDM sphere (a), the 225 nm diameter single MDM sphere (b), and the particle of these coupled spheres (c). and insets demonstrate 3D radiation pattern diagrams at the particular frequency.

resonance or lower than magnetic resonance. But corresponding to these forward scattering sections are very low. From Fig. 2(c), the coupled particles show two distinct peaks in its f/b ratio (attain about 40) spectra at 790 THz and 950 THz, respectively. But compared with the scattering efficiency at 790 THz, the scattering efficiency at 950 THz is very low similarly. The f/b ratio of the coupled particles attains about 40 at 790 THz with the forward scattering attained a peak and backward scattering was suppressed. Fig. 2 also shows 3D radiation pattern diagrams at the frequencies of maximum f/b ratios. The scattering intensity of the asymmetric dimer in the forward direction (along the z axis) is more than 12, which is larger than two single particles. This enhancement in intensity clearly exhibited the merit of the asymmetric MDM dimer which can fully utilize the scattering resonance for unidirectional forward scattering. In addition, these corresponding beam-width of the main lobes are 40.9 deg, 40.3 deg, and 30.6 deg. It is obvious that the MDM dimer has more narrow beam-width of the main lobes compared with the individual particle owing to the magnetic high-order multipoles, which response to the excitation of the plane wave in the particle, and the magnetic high-order multipoles can contribute to improve the directivity and narrow the radiation beam. According to the 3-D radiation diagram, these main lobes of the coupled particles are extremely narrow, and the backward radiation almost vanished at these frequencies. The small fraction of the backward scattering is observed in the far-field 3-D radiation diagram of the particle, possibly due to the presence of magnetic octupoles excited in the smaller particle. It is clearly showed that the advantage of the asymmetric MDM particle which can improve the properties of unidirectional forward scattering.

It is all know that metallic nanoantennas have large power absorption and substantial energy loss at optical frequency. Because losses arising from interband transitions occur when a valence electron in the metal absorbs a photon to jump to the Fermi surface or when an electron near the Fermi surface absorbs a photon to jump to the next unoccupied state in the conduction band [31], [32]. However, this nanoantenna of MDM dimer structure presents a broad scattering resonance around 790 THz, furthermore, the low-energy band gap of Ge, and low absorption of Ag lead to a very low absorption in this region as shown in the Fig. 3(a).

Figure 3(b) illustrates the near-field electric distribution around the MDM dimer excited at 790 THz. The typical enhancement of electric field near the metal shell and core, which correspond to electric and magnetic resonances, were observed in the small and large spheres respectively. The electric localized surface plasmon resonances are observed not only in the large particle showed not only an $x-$ component but also a $z-$ component, resulting from an electric resonance along the $z-$ axis is induced by the interaction with the magnetic resonance of the small particle [20]. Intense confinement and enhancement of the electric field are generated in the large sphere and small sphere respectively, suggesting the presence of coupling between the electric and magnetic near-field resonances of each sphere. The intensity of the hot spot does not generate at the gap, which results in the particle having a high f/b ratio even the couple particles are not placed very close.

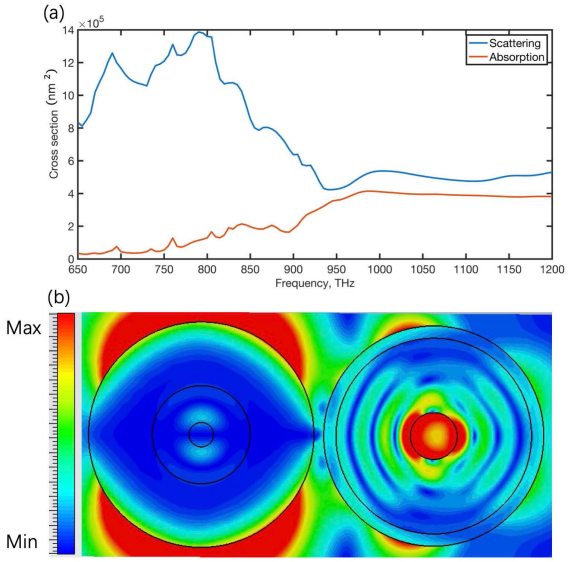

FIGURE 3. (a) Numerical calculation results showing a low absorption cross section for the particle at 790 THz. (b) Near-field electric distribution map for the asymmetric MDM particle in the plane normal to k and parallel to the particle axis excited at 790 THz.

We show the result of eq 1 in Fig. 4 with the gap separation of 40 nm. The result of far-field scattering spectra which is calculated by using the theoretical model based on the dipole-dipole model and has some differences with the full numerical electrodynamical calculations performed using the FDTD method. Because the first method based on dipole-dipole interaction, these multipolar contributions obtained in the FDTD calculations are not shown in the results

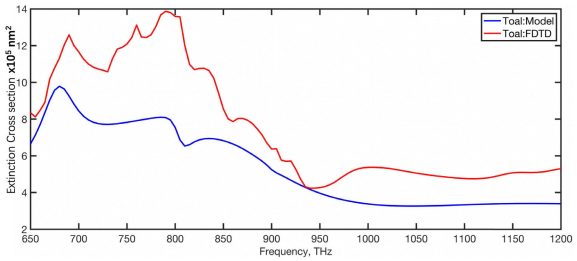

FIGURE 4. Theoretical analysis of scattering spectra of two interacting electric and magnetic dipoles using the dipole-dipole model for coupling situation is compared with the FDTD results, for the gap separation of 40 nm.

included in the simple model. And its allow us to calculate separately the contribution of each interaction to the total scattering cross-section of the particle. The feature around 680 THz can be identified as the magnetic dipole- magnetic dipole interaction given by in the first equation. And the differences between the dipole-dipole model and FDTD are lager at 790 THz owing to the only dipole contribution come from the larger particle and the small particle support litter dipole moment.

We now show the responses of the nanoantenna with different gaps separation of the dimer. Fig. 5 (c) shows the f/b ratio of the asymmetric particle with the gap from 5nm to 150nm. The f/b ratio attains high value at 790 THz and 950 THz when the gap is smaller than 15 nm due to the near-field induced electric dipole-magnetic dipole interaction supports a substantial contribution to the total scattering cross-section when the separation of the gap is small. But the scattering efficiency of the particle is very low (under

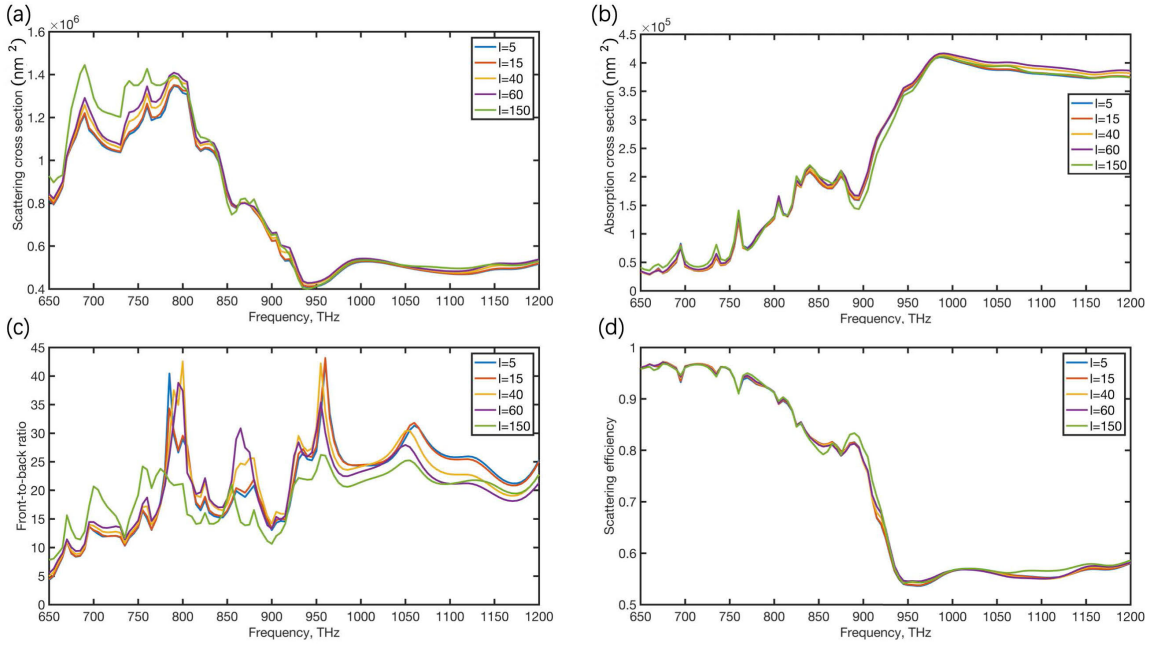

FIGURE 5. Scattering (a) and absorption (b) cross-section and f/b ratio (c) scattering efficiency (d) as a function of the gap separation of the asymmetric particle.

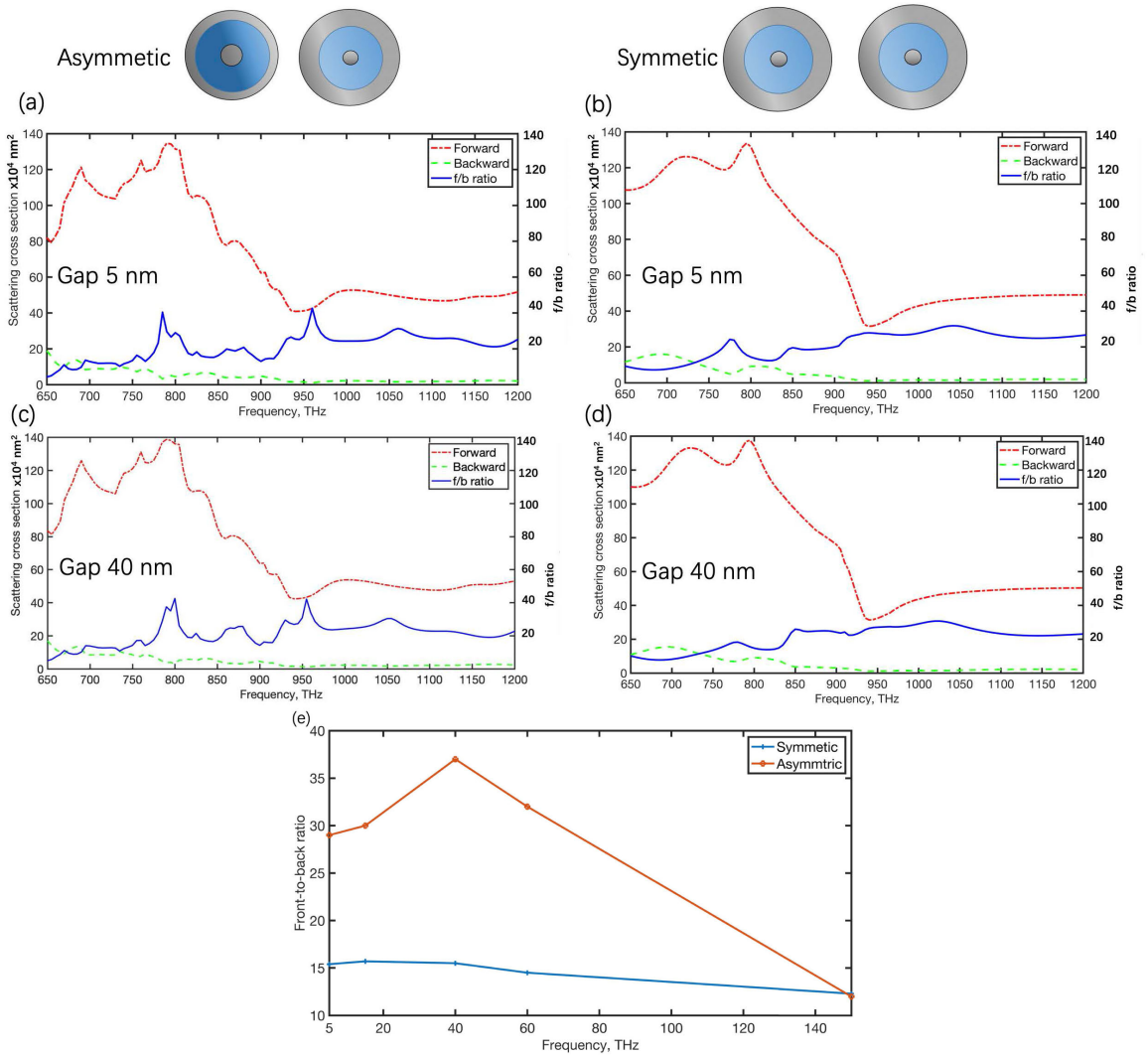

FIGURE 6. Comparison between asymmetric and symmetric particle structures. (a, b) the scattering cross section to the forward and backward direction and the f/b ratio of the asymmetric particle (a) and symmetric particle (b) with the gap separation of 5 nm. (c, d) the scattering cross section to the forward and backward direction and the f/b ratio of the asymmetric particle (c) and symmetric particle (d) with the gap separation of 40 nm. (e) f/b ratio as a function of the gap separation of asymmetric and symmetric particles.

60%) at 950 THz owing to lager absorption in the metal. In general, the high f/b can be reached only when the coupled particles are placed very close (the gap is smaller than 40 nm) to each other. However, this contribution is not so important in this MDM dimer. The f/b ratio of this asymmetric dimer can surpass 20 even the gap exceeds 150 nm at 790 THz which is also shown in Fig. 5 (c). The f/b ratio peaks of the asymmetric dimer dropped litter when the gap increased to 60 nm, however, the f/b ratio peak is shifted as the gap exceeded 60 nm owing to the strength of near field decreases as the particles move apart. Furthermore, the scattering and absorption cross-section and scattering efficiency are also shown in Fig. 5 a-b, for the gap from 5 nm to 150 nm. With the litter separation of gap (low than 60 nm), the forward scattering cross-section was almost the same which have a resonant peak at 790 THz. Both the scattering and absorption cross-section of the asymmetric dimer showed little change when the separation of gap did not exceed 60 nm. However, if the separation of gap up to or beyond 150 nm for the larger gap, the forward scattering cross-section resonant peak of the particle has changed to frequencies of 690 THz and 760 THz with the high f/b ratio in 760 THz. The asymmetric dimer presents broad scattering resonance at 650-850 THz when the absorption is low. This behavior with the separation of gap size changing due to this nanostructure is not necessary to get strong coupling and also can have the better f/b ratio when the dimer shows the broadening of the electric mode, and the fulfillment of the high f/b ratio condition requires the overlap of the independent electric and magnetic resonances which becomes less dependent on the strong coupling [33]. The nanoantenna with different diameters of gaps can result in different work characteristics. And the fabrication of this

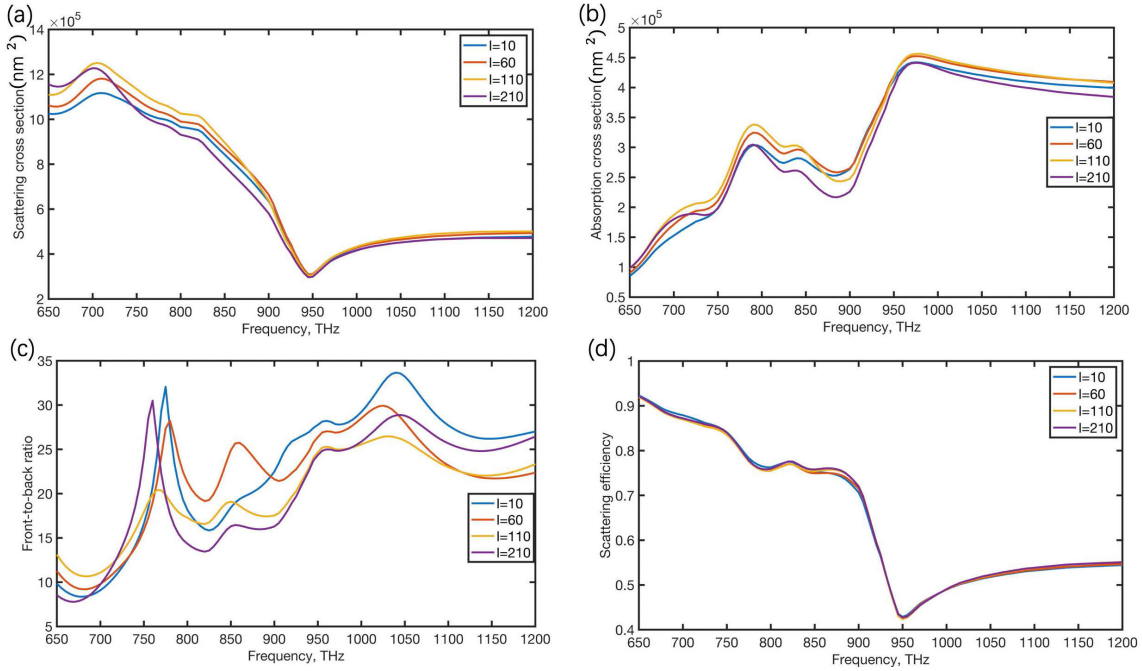

FIGURE 7. Scattering (a) and absorption (b) cross-section, f/b ratio (c) and scattering efficiency (d) as a function of the gap separation of the asymmetric particle consisting of 225 nm and 230 nm diameter Ag sphere.

nanoantenna would be difficult if this nanostructure antenna needs to keep the gap between two particles so close. This nanoantenna does not need to keep the separation gap of the particle so small and it's f/b ratio can surpass 20 even the gap exceeds 150 nm. These results show that this nanostructure antenna can be much more easily applied to practical application.

We now compare our asymmetric dimer configuration with a symmetric one. The scattering cross-section and f/b ratio of an asymmetric dimer of 225 nm and 230 nm diameter MDM nanoparticles and of a symmetric dimer of 230 nm diameter nanoparticles are shown in Fig. 6 (a-d), for the gap of 5 nm or 40 nm. These forward scattering cross-section of both nanoantennas have the same resonant peak at 790 THz. While the f/b ratio of the asymmetric dimer at the resonant maximum is about two times than the symmetric one. For the larger gap, the forward scattering of both nanoantennas and the f/b ratio of the symmetric dimer showed litter change, but the f/b ratio of the asymmetric one attain 40, showing more separation from each other.

Fig. 6(e) shows the f/b ratio at the forward scattering maximum as a function of the gap separation for both nanoantennas. As the gap increased, the f/b ratio of the asymmetric dimer attains maximum value when the gap is 40 nm and the f/b ratio is dropping with the gap being larger than 40 nm. In contrast, the f/b ratio of the symmetric dimer dropped slowly with low value. These differences in behavior with gap size are due to effectively coupled electric dipole mode and magnetic multiple modes in the asymmetric dimer.

We also show the response of the nanoantenna with different separation gaps consisting of two Ag particles. Both the scattering and absorption cross-section of the asymmetric particle showed little change when the separation of the gap is increased which is shown in Fig. 7(a) and Fig. 7(b) respectively. The asymmetric dimer with Ag spherical particles presents scattering resonance at 700 THz with the low f/b ratio (under 10). The coupled Ag particles with a separation gap of 10 nm attain 33 f/b ratio at 1030 THz but the forward scattering attained a drop and the scattering efficiency is about 50% owing to large absorption in Ag material. As the separation of gap up to 210 nm for the larger gap, the f/b ratio peak attain about 25 at 1030 THz which is shown in Fig. 7(c). Fig. 7(c) also shows that another f/b ratio peak at 760 THz with the forward scattering did not attain a peak and the scattering efficiency is about 75%. Furthermore, the scattering efficiency has litter change results from the separation gap increasing (Fig. 7(d)). Comparing with the MDM particle, the Ag particle cannot get the maximum f/b ratio with the scattering resonance and low loss. These clearly demonstrate that the effect of the maximum f/b ratio and scattering resonance in such a system requires core-dual shells nanostructural.

IV. CONCLUSION

To conclude, we have proposed a novel optical nanoantenna, consisting of an asymmetric dimer of two core-dual shells spheres excited by a plane wave source polarization perpendicular to the dimer axis in the air. These radiative properties of the asymmetric dimer are analyzed by the dipole-dipole

theory [20] and the 3-D numerical calculation. Results indicate that the asymmetric dimer can generate broaden scattering resonance with low absorption, and have the high f/b ratio with narrow beam-width of the main lobes. The high f/b ratio of this nanoantenna can be enhanced via decreasing the gap separation distance for the asymmetric dimer have been further demonstrated. In addition, this nanostructure antenna does not need to keep the separation gap of the particle so small and it's f/b ratio can surpass 20 even the gap exceeds 150 nm at 790 THz. Comparing with the symmetric dimer and the pure metal coupled asymmetric particles, the proposed nanoantenna may exhibit higher directivity and low loss respectively, due to effectively coupled electric dipole mode and magnetic multipole mode. Such design integrates the advantages of array dielectric nanoantenna and plasmonic nanoantenna such as the high f/b ratio, narrow beam-width, low loss, emission direction control, and highly localized excitation enhancement based on the excitation of electric dipole mode and magnetic high-order mode and makes them coupling in the gap effectively. Our findings show the aligned metal-dielectric-metal nanoparticles can act as low-loss nanoantennas which can control light with high directivity, and boost realization of practical metasurface and nanometer scale devices using optical nanoantennas.

REFERENCES

[1] H. Shi, J. Li, A. Zhang, J. Wang, and Z. Xu, "Broadband cross polarization converter using plasmon hybridizations in a ring/disk cavity," *Opt. Express*, vol. 22, no. 17, pp. 20973–20981, 2014.

[2] L. Shi, P. Pottier, Y.-A. Peter, and M. Skorobogatiy, "Guided-mode resonance photonic crystal slab sensors based on bead monolayer geometry," *Opt. Express*, vol. 16, no. 22, pp. 17962–17971, 2008.

[3] Y.-L. Zhang, R. P. H. Wu, A. Kumar, T. Si, and K. H. Fung, "Nonsymmorphic symmetry-protected topological modes in plasmonic nanoribbon lattices," *Phys. Rev. B, Condens. Matter*, vol. 97, no. 14, pp. 144–203, 2018.

[4] L. Shi, A. Kabashin, and M. Skorobogatiy, "Spectral, amplitude and phase sensitivity of a plasmonic gas sensor in a metallic photonic crystal slab geometry: Comparison of the near and far field phase detection strategies," *Sens. Actuators B, Chem.*, vol 143, no. 1, pp. 76–86, Dec. 2009.

[5] H. Shi, J. Li, A. Zhang, Y. Jiang, J. Wang, Z. Xu, and S. Xia, "Gradient metasurface with both polarization-controlled directional surface wave coupling and anomalous reflection," *IEEE Antennas Wireless Propag. Lett.*, vol. 14, pp. 104–107, 2014.

[6] D. Huang, L. Yang, H. Cao, Z. Meng, Y. Tian, and X. Tan, "Unidirectional optical nanoantenna with individual core–dual shells nanoparticle," *J. Nanophoton.*, vol. 12, no. 4, 2018, Art. no. 046005.

[7] C. Huang, W. Pan, X. Ma, and X. Luo, "1-bit reconfigurable circularly polarized transmitarray in X-band," *IEEE Antennas Wireless Propag. Lett.*, vol. 15, pp. 448–451, Jul. 2015.

[8] S. A. Maier, *Plasmonics: Fundamentals and Applications*. Springer, 2007.

[9] D. K. Gramotnev and S. I. Bozhevolnyi, "Plasmonics beyond the diffraction limit," *Nature Photon.*, vol. 4, no. 2, pp. 83–91, 2010.

[10] T. H. Taminiau, F. D. Stefani, and N. F. van Hulst, "Enhanced directional excitation and emission of single emitters by a nano-optical Yagi-Uda antenna," *Opt. Express*, vol. 16, no. 14, pp. 10858–10866, 2008.

[11] T. Shegai, S. Chen, V. D. Miljković, G. Zengin, P. Johansson, and M. Käll, "A bimetallic nanoantenna for directional colour routing," *Nature Commun.*, vol. 2, p. 481, Sep. 2011.

[12] D. Vercruysse, Y. Sonnefraud, N. Verellen, F. B. Fuchs, G. Di Martino, L. Lagae, V. V. Moshchalkov, S. A. Maier, and P. Van Dorpe, "Unidirectional side scattering of light by a single-element nanoantenna," *Nano Lett.*, vol. 13, no. 8, pp. 3843–3849, 2013.

[13] J. A. Schuller and M. L. Brongersma, "General properties of dielectric optical antennas," *Opt. Express*, vol. 17, no. 26, pp. 24084–24095, 2009.

[14] D. S. Filonov, A. E. Krasnok, A. P. Slobozhanyuk, P. V. Kapitanova, E. A. Nenasheva, Y. S. Kivshar, and P. A. Belov, "Experimental verification of the concept of all-dielectric nanoantennas," *Appl. Phys. Lett.*, vol. 100, no. 20, 2012, Art. no. 201113.

[15] A. E. Krasnok, A. E. Miroshnichenko, P. A. Belov, and Y. S. Kivshar, "All-dielectric optical nanoantennas," *Opt. Express*, vol. 20, no. 18, pp. 20599–20604, 2012.

[16] L. Zou, W. Withayachumnankul, C. M. Shah, A. Mitchell, M. Bhaskaran, S. Sriram, and C. Fumeaux, "Dielectric resonator nanoantennas at visible frequencies," *Optics Express*, vol. 21, no. 1, pp. 1344–1352, 2013.

[17] H.-S. Ee, J.-H. Kang, M. L. Brongersma, and M.-K. Seo, "Shape-dependent light scattering properties of subwavelength silicon nanoblocks," *Nano Lett.*, vol. 15, no. 3, pp. 1759–1765, 2015.

[18] W. Liu, "Ultra-directional super-scattering of homogenous spherical particles with radial anisotropy," *Opt. Express*, vol. 23, no. 11, pp. 14734–14743 2015.

[19] X. Zhang, J.-J. Xiao, Q. Zhang, F. Qin, X. Cai, and F. Ye, "Dual-band unidirectional emission in a multilayered metal–dielectric nanoantenna," *ACS Omega*, vol. 2, no. 3, pp. 774–783, 2017.

[20] P. Albella, M. A. Poyli, M. K. Schmidt, S. A. Maier, F. Moreno, J. J. Sáenz, and J. Aizpurua, "Low-loss electric and magnetic field-enhanced spectroscopy with subwavelength silicon dimers," *J. Phys. Chem. C*, vol. 117, no. 26, pp. 13573–13584, 2013.

[21] T. Shibanuma, P. Albella, and S. A. Maier, "Unidirectional light scattering with high efficiency at optical frequencies based on low-loss dielectric nanoantennas," *Nanoscale*, vol. 8, no. 29, pp. 14184–14192, 2016.

[22] M. Caldarola, P. Albella, E. Cortés, M. Rahmani, T. Roschuk, G. Grinblat, R. F. Oulton, A. V. Bragas, and S. A. Maier, "Non-plasmonic nanoantennas for surface enhanced spectroscopies with ultra-low heat conversion," *Nature Commun.*, vol. 6, Aug. 2015, Art. no. 7915.

[23] N. Noginova, Y. Barnakov, H. Li, and M. A. Noginov, "Effect of metallic surface on electric dipole and magnetic dipole emission transitions in Eu^{3+} doped polymeric film," *Opt. Express*, vol. 17, no. 13, pp. 10767–10772, 2009.

[24] S. Karaveli and R. Zia, "Spectral tuning by selective enhancement of electric and magnetic dipole emission," *Phys. Rev. Lett.*, vol. 106, no. 19, 2011, Art. no. 193004.

[25] L. Aigouy, A. Cazé, P. Gredin, M. Mortier, and R. Carminati, "Mapping and quantifying electric and magnetic dipole luminescence at the nanoscale," *Phys. Rev. Lett.*, vol. 113, no. 7, 2014, Art. no. 076101.

[26] A. García-Etxarri, R. Gómez-Medina, L. S. Froufe-Pérez, C. López, L. Chantada, F. Scheffold, J. Aizpurua, M. Nieto-Vesperinas, and J. J. Sáenz, "Strong magnetic response of submicron silicon particles in the infrared," *Opt. Express*, vol. 19, no. 6, pp. 4815–4826, 2011.

[27] A. I. Kuznetsov, A. E. Miroshnichenko, Y. H. Fu, J. Zhang, and B. Luk'yanchuk, "Magnetic light," *Sci. Rep.*, vol. 2, Jul. 2012, Art. no. 492.

[28] C. F. Bohren and D. R. Huffman, *Absorption and Scattering of Light by Small Particles*. Hoboken, NJ, USA: Wiley, 1983.

[29] O. Peña-Rodríguez, A. Rivera, M. Campoy-Quiles, and U. Pal, "Tunable Fano resonance in symmetric multilayered gold nanoshells," *Nanoscale*, vol. 5, no. 1, pp. 209–216, 2013.

[30] P. B. Johnson and R. W. Christy, "Optical constants of the noble metals," *Phys. Rev. B, Condens. Matter*, vol. 6, no. 12, p. 4370, 1972.

[31] J. B. Khurgin and A. Boltasseva, "Reflecting upon the losses in plasmonics and metamaterials," *MRS Bull.*, vol. 37, pp. 768–779, Aug. 2012.

[32] G. V. Naik, V. M. Shalaev, and A. Boltasseva, "Alternative plasmonic materials: Beyond gold and silver," *Adv. Mater.*, vol. 25, pp. 3264–3294, Jun. 2013.

[33] P. Albella, T. Shibanuma, and S. A. Maier, "Switchable directional scattering of electromagnetic radiation with subwavelength asymmetric silicon dimers," *Sci. Rep.*, vol. 5, Dec. 2015, Art. no. 18322.

[34] L. Novotny and N. van Hulst, "Antennas for light," *Nature Photon.*, vol. 5, no. 2, pp. 83–90, 2011.

[35] V. Giannini, A. I. Fernández-Domínguez, S. C. Heck, and S. A. Maier, "Plasmonic nanoantennas: Fundamentals and their use in controlling the radiative properties of nanoemitters," *Chem. Rev.*, vol. 111, no. 6, pp. 3888–3912, 2011.

DENGCHAO HUANG received the B.S. degree in electronic information engineering from Sanlian College, Heifei, China, in 2012, and the M.S. degree in communication engineering from the Yunnan University of Nationalities, Kunming, China, in 2016. He is currently pursuing the Ph.D. degree in circuit and systems with the Institute of Aerocraft Tracking, Microelectronics and Communications Engineering, Chongqing University, Chongqing, China.

His research interests include wireless sensor networks, metamaterials, and optical antenna.

YI ZHANG received the B.S. degree in electronic information engineering and the M.S. degree in communication and system from Chongqing University, Chongqing, China, in 2013 and 2016, respectively, where he is currently pursuing the Ph.D. degree in circuit and systems with the Institute of Aerocraft Tracking, Microelectronics and Communications Engineering.

His research interests include wireless sensor networks, metamaterials, and optical antenna.

LISHENG YANG received the B.S. degree in radio technology, and the M.S. and Ph.D. degrees in circuit and systems from Chongqing University, Chongqing, China, in 1992, 2004, and 2006, respectively.

He has been a Researcher and a Doctoral Supervisor with the Institute of Aerocraft Tracking, Microelectronics and Communications Engineering, Chongqing University. From 2004 to 2005, he was the Key Innovation Platform of the National "985 Project" and responsible for the research on formation flight satellite measurement and control system of the China Academy of Aerospace Science and Industry Information Technology. Since 2005, he has been the backbone of the CNGI Project of the National Development and Reform Commission, responsible for the research and development of the cngi-ap multi-user smart antenna system. As a key expert in the National "985 Project" Key Innovation Platform tt&c and Remote Sensing Information Transmission Research Institute/Multi-Target tt&c and High-Precision tt&c Research Center, he participated in the research and development of special communication system, a major military project of the ninth five-year plan of the general staff. He was supported by the New Century Excellent Talents Support Program of the Ministry of Education, in 2007. His research interests include 5G, software radio, wireless sensor networks, and metamaterials.

Dr. Yang's awards and honors include the Second Prize of the National Science and Technology Progress Award, in 2004, and the Third Winner.